Semi-Insulating III-V Materials, © Ohmsha, Ltd. 1986

Application of Modern Magnetic Resonance Techniques to the Characterization of Point Defects in Semi-Insulating III-V Semiconductors

J.-M. SPAETH

University of Paderborn, Fachbereich 6, Physik,
Warburger Str. 100A, 4790 Paderborn, F.R.G.

ABSTRACT

Recent developments in the application of multiple magnetic resonance techniques to the determination of the structure of point defects in III-V semiconductors are briefly reviewed. Major features are illustrated with yet unpublished results on the Ga-vacancy in GaP and the anion antisite defects (As_{Ga}) in GaAs. The relation of the antisites to EL2 defects derived from photoquenching and magnetic resonance excitation spectroscopy are briefly discussed.

1. INTRODUCTION

For a characterization of a point defect in semiconductors one needs to know its microscopic (atomic) structure, its electronic structure and the energy level position in the gap as fundamental features. In the case of paramagnetic defects the first two features can in principle be derived from magnetic resonance experiments. In practice, however, electron spin resonance (ESR) can yield this only in particularly favourable cases, where the hyperfine (hf) and in particular the ligand hf interactions can be resolved. In general, one has to resort to electron nuclear double resonance (ENDOR) experiments to achieve this (1-4). ENDOR spectra are mostly complicated and not easy to measure nor to analyse. In recent years progress was made by computer assisted experiments and the application of advanced ENDOR techniques like ENDOR-induced ESR (5) and DOUBLE-ENDOR (6). Some of the salient features of this development will be summarized and illustrated with unpublished results on the Ga-vacancy in GaP.

Optical detection of magnetic resonance is an established highly sensitive technique for semiconductors using the donor-acceptor recombination fluorescence (7). However, no ENDOR experiments with this technique were reported with resolved ligand hf interactions. Recently, in GaAs, by measuring the optical detection of magnetic resonance via the magnetic circular dichroism of the absorption, a technique developed originally for the study of colour centres in ionic crystals (8), not only a high sensivity could be achieved for ESR (9), but also ENDOR could be measured with resolution of the ligand hf interactions of several neighbour shells (10). The method will be briefly explained and new results on the anion antisite defects in GaAs will be presented. By measuring the photo-excitation spectrum of the optically detected ESR and ENDOR spectra and the photoquenching behaviour it could be shown that the As_{Ga}-As_i complex identified to be the 'antisite' defect in as-grown s.i. GaAs has the same optical and photoquenching properties as the EL2 defect and can therefore be identified with it.

2. COMPUTER-ASSISTED ELECTRON NUCLEAR DOUBLE RESONANCE (ENDOR)

From the symmetry of the ligand hf interactions one can determine the site of the defect, from the size the electronic structure. For impurity centres the hf interaction with the central nucleus allows its chemical identification. The ligand hf structure can be resolved by ENDOR experiments, in which the nuclear magnetic resonance (NMR) transitions of nuclei coupled to the unpaired electron(s) are detected by measuring the change of the partly saturated ESR transition (11). A direct detection of the NMR is not possible. The double resonance experiment gives a sensitivity enhancement of several orders of magnitude compared to NMR and a hf resolution enhancement compared to ESR. The spin Hamiltonian for the paramagnetic defect is

$$H = \mu_B \vec{B}_o \tilde{\tilde{g}} \vec{S} + \sum_{\alpha=a}^{n} (\vec{I}_\alpha \tilde{A}_\alpha \vec{S} + \vec{I}_\alpha \tilde{Q}_\alpha \vec{I}_\alpha - g_{I,\alpha} \mu_n \vec{B}_o \vec{I}_\alpha) \qquad (1)$$

It contains the electron Zeeman, hf, quadrupole and nuclear Zeeman energies. The sum runs over the central nucleus and all interacting ligands (12). The ENDOR (NMR) frequencies are given in first order perturbation theory by

$$\nu(m_s) = \frac{1}{h} \left| m_s(a+b(3\cos^2\gamma - 1) \mp g_I \mu_n B_o \pm 3m_q \cdot q(3\cos^2\gamma' - 1) \right| \qquad (2)$$

where the isotropic hf constant a and the anisotropic hf constant b and the quadrupole constant q are related to their respective tensors by

$$A_{zz} = a+2b, \quad A_{xx} = A_{yy} = a-b, \quad Q_{zz} = 2q, \quad Q_{xx} = Q_{yy} = -q \qquad (3)$$

γ and γ' are the angles between the principal axes with the largest interaction and the magnetic field. $m_q = (m_I + m_I')/2$, the average between the two nuclear spin quantum numbers, which are connected by the NMR transition (11,13). For simplicity, axially symmetric tensors are assumed.

Without quadrupole interaction each ligand nucleus gives rise to $(2m_s+1)$ ENDOR lines. With quadrupole interaction this number is multiplied according to equ.(2). To determine the site symmetry of the defect and the ligand interaction constants one has to measure and analyse the angular dependence of the ENDOR lines. The approximation of equ.(2) holds only for simple cases and was not applicable in III-V semiconductors (1-3). For Ni^{3+} in GaP for each crystal orientation more than 500 ENDOR lines appeared and for their analysis the angular dependence had to be measured in very small angular steps (3). Such experiments are only feasible by using computer assisted ENDOR spectrometers for automised measurements of the angular dependence.

Digitial filters can be applied to the spectra to improve the signal to noise ratio (14). The frequency positions of the lines are determined by applying special peak search algorithms and deconvolution procedures (15).

Fig. 1 shows as a recent example a section of the high frequency ENDOR angular dependence of the Ga-vacancy in GaP. Its ESR spectrum was first investigated by Kennedy and Wilsey (16). Already a rough analysis according to equ.(2) confirmed that S = 3/2, as was proposed earlier from ESR experiments under uniaxial stress (17), and that the ENDOR lines of Fig. 1 are due to nearest P-neighbours (I = 1/2). However, if one assumes a perfect tetrahedral symmetry and solves equ.(1) in perturbation theory to 2nd order including the effect of pseudo-dipolar coupling of the 4 nearest P nuclei via their isotropic hf interaction (18), one cannot explain the high number of lines in Fig. 1. The small observed splittings are suggestive of a slight distortion of the defect, which would then be measured in various orientations simultaneously, giving rise to more ENDOR lines. It was excluded by ENDOR-induced ESR experiments, a kind of ENDOR-line excitation spectroscopy, that different defects are superimposed in the ESR spectrum causing additional ENDOR lines (5). The experimental proof, that the defect has indeed perfect

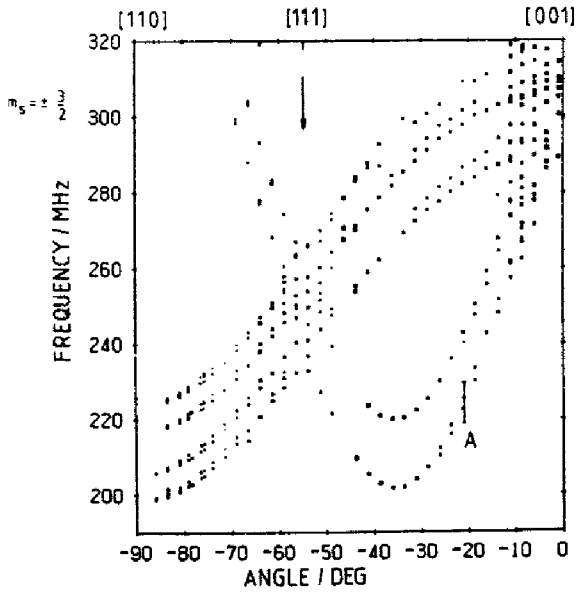

Figure 1 Part of the angular dependence of ENDOR lines of nearest P-neighbours of the Ga-vacancy in GaP. The magnetic field was rotated in a (110)-plane (X-band).

tetrahedral symmetry, could be given by performing DOUBLE-ENDOR experiments (triple resonance). Two NMR frequencies are applied simultaneously and the influence of one ENDOR transitions to the 2nd one is monitored. There is a signal only, if both nuclei belong to the same defect. Otherwise, they are not coupled. A DOUBLE-ENDOR signal is measured only, if both nuclei belong to the same defect orientation in case of low symmetry defects (6). Fig. 2 shows the ENDOR and DOUBLE-ENDOR spectrum for B_o near [111]. In both spectra all lines appear proving that the vacancy is not a low symmetry defect. The occurence of so many lines proved to be the result of a coupling between the different P-neighbour nuclei, which could be understood quantitatively by diagonalising the spin Hamiltonian numerically. The additional splittings compared to earlier treatments of this effect (18) are due to the large anisotropic part of the ligand hf interaction. Thus, the Ga-vacancy has S = 3/2, perfect tetrahedral symmetry and the interaction parameters a = 195 MHz, b = 54.5 MHz for the nearest P-neighbours. The interaction with one more P and one Ga shell could also be resolved (4).

3. OPTICAL ABSORPTION DETECTED ESR AND ENDOR

The detection of ESR and ENDOR via the optical absorption is based on its magnetic circular dichroism (MCD). In Fig. 3a a simplified free atom model for an s→p transition in a magnetic field presents the essential features. In a crystal the two circular polarised absorption transitions σ_+ and σ_- are, of course, phonon broadened. The MCD, proportional to the difference $(\sigma_+ - \sigma_-)$, is approximately the derivative of the absorption band, if the spin orbit splitting $\Delta_{s,o.}$ in the excited state is smaller than the band width. Its peak separation is given by $\Delta_{s.o.}$ (see Fig. 3b). The peak heights of the MCD are given by (19)

$$MCD_{extr} \propto \Delta_{s.o.} \frac{n_- - n_+}{n_- + n_+} \propto \Delta_{s.o.} \tanh \frac{g_e \mu_B B_o}{2kT} \qquad (4)$$

A variation of the relative population numbers n_+ and n_- of the electronic Zeeman levels changes the MCD. By ESR transitions the difference in $(n_- - n_+)$ is diminished provided the spin lattice relaxation time T_1 is long enough to allow a partial saturation of this transition. By monitoring the decrease of MCD_{extr} the ESR transition can be detected.

An unexpected successful application of this technique was obtained in undoped, semiinsulating 'as-grown' GaAs, although in the optical absorption spectrum no absorption can be detected apart from the very weak EL2 band at 1.18 eV. There is a relatively large MCD between 900 and 1500 nm, which has the shape of two superimposed derivative structures (9). The ODESR spectrum found was the well known 4 line 'finger-print' spectrum of the anion antisite defects As_{Ga}, the 4 line hf splitting being due to a central ^{75}As nucleus

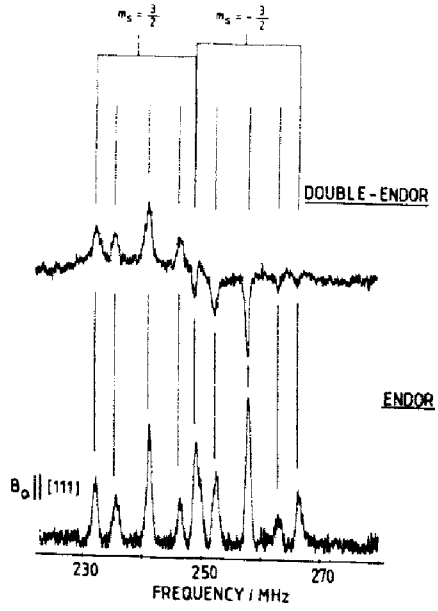

Figure 2 ENDOR and DOUBLE-ENDOR spectrum of nearest P-neighbour lines of the Ga-vancancy in GaP for B_0 approx. parallel to [111].

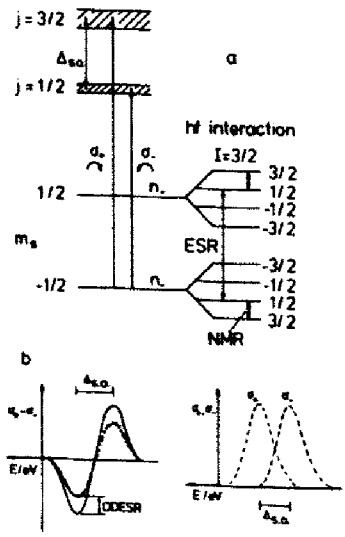

Figure 3 Simplified level scheme to explain the magnetic circular dichroism of the absorption and the optical detection of the electron spin resonance and electron nuclear double resonance (not to scale).

(I = 3/2). The signal to noise ratio was 2 orders of magnitude better than that of conventional ESR. However, both spectra differed in T_1 indicating that the As_{Ga} defects measured optically and conventionally must differ in structural details (20,21). No ligand hf structure is resolved in the ESR spectrum. Conventional ENDOR experiments were not possible due to the weak ESR spectrum. With optical detection ENDOR experiments were successful (10). Through the ligand hf interactions the level scheme is more complicated than that shown inf Fig. 3a. Each of the central ^{75}As nuclear Zeeman levels is further split. In order to explain the principle of the mechanism to detect ENDOR optically, it is assumed for simplicity that the hf pattern in Fig. 3a is due to one As ligand. Since in an allowed ESR transition no nuclear spins must flip (12), each ESR transition causes only a partial decrease of the MCD, in the simplified example only 1/4 of the total decrease possible. If simultaneously an NMR transition is induced additional populations of the nuclear Zeeman levels are included in the ESR transition and hence the decrease of the MCD is stronger. Thus, the change of the ODESR detects the NMR transition (10). Fig. 4 shows a section of the ENDOR spectrum of antisite defects in an undoped 'as-grown' (pBN-LEC) s.i. GaAs sample (from MRC), as it was recently measured. The signal is the change of the ODESR effect as a function of the NMR frequencies. The signal to noise ratio of the ENDOR effect is of the same order of magnitude as that of the ODESR effect, a definite advantage over the conventional ENDOR method. Fig. 5 shows the angular dependence between 40 - 100 MHz. There are more lines below and above that range. The recent measurements are greatly improved compared to first results given in ref. 10 due to better experimental conditions and more experience with this kind of experiment. The width of the ENDOR lines turned out to be smaller here as well as in a V-doped sample compared to the Cr-doped s.i. sample used in ref. 10. Many more NMR transitions could be detected.

The lines of Fig. 5 belong to nearest ^{75}As neighbours. A regular antisite defect with 4 tetrahedrally coordinated ^{75}As neighbours would have far less ENDOR lines according to equ.(2). However, quite similarly as in the case of the Ga-vacancy in GaP, the 4 nearest neighbours interact via a pseudo-dipolar coupling, which leads to numerous line splittings. There is a large anisotropic

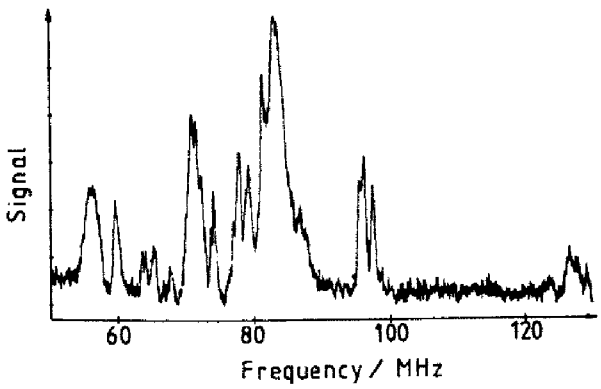

Figure 4 Part of the optically detected ENDOR spectrum of anion antisite defects in s.i. as-grown, undoped GaAs for B_o in a (110)-plane. T=1,5K, ν = 24 GHz.

hf interaction and a quadrupole interaction. The angular pattern can be understood by numerical diagonalisation of equ.(1). However, there are also ENDOR lines above 100 MHz (see Fig. 4), which can be shown to belong to the same defect. They are also due to ^{75}As, namely tue to one interstitial As atom in the tetrahedral interstitial site. It has [111]-symmetry with respect to the central atom. The ODENDOR experiments show that the antisite defects are complexed with As, that is they are $AsAs_4$-As_i complexes. The same spectra were found so far also in a V-doped and another undoped sample (22).

4. CORRELATION OF ESR/ENDOR WITH OPTICAL BANDS AND ENERGY LEVEL POSITIONS

When B_o is set to one particular ODESR line or the NMR frequency to one particular ODENDOR line and these ESR/ENDOR lines are than monitored as a function of the optical wavelength, one measures that part of the MCD, which belongs to this particular paramagnetic defect ("MCD-tagged by ESR or ENDOR") (23). For the antisite spectra in 'as-grown' material it was found that the total MCD measured belongs to it (9,10).

A correlation with the energy level positions can be made by photo-ODESR/ODENDOR. In p-type GaAs:Zn (HB, MCP Ltd., $p \sim 4 \cdot 10^{16} cm^{-3}$) the paramagnetic antisite $D^+/^{++}$ level is empty, since the Fermi level is close to the Zn acceptors. No As_{Ga}-MCD can be observed. Upon additional light excitation the level could be populated from the valence band. For light with energy $h\nu$ > = 0.52 eV. For light energies above 0.73 eV the intensity decreased again, upon which an absorption band peaking at 1.2 eV appeared, which is identical with the band ascribed to the EL2 defects. A photo-ODENDOR experiment showed, that the ODESR spectrum is due to the $AsAs_4$-As_i complex. These experiments show that the energy levels of the $AsAs_4$-As_i complex are E_v + 0.52 eV (D^+/D^{++}) and E_v + 0.73 eV (D^o/D^+). The The appearance of the 1.2 eV absorption band and the EL2 like photoquenching behaviour led to the conclusion that the neutral, isolated As_{Ga}-A_i complex (diamagnetic) can be associated with one of the EL2 defects (24).

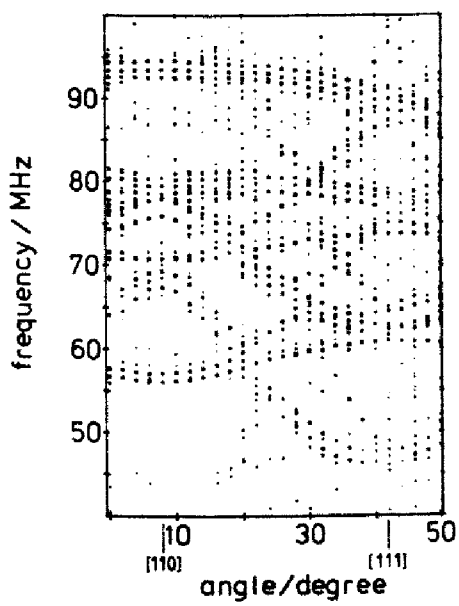

Figure 5 Part of the angular dependence of ODENDOR lines of anion antisite defects in s.i. as-grown undoped GaAs for rotation of B_o in a (110)-plane.

REFERENCES

1. Teuerle W. and Hausmann A (1976). J. Phys. B23,11
2. Hage J., Niklas J.R. and Spaeth J.-M. (1985). J. Electr. Mat. 14a, 1051
3. Ueda Y., Niklas J.R., Spaeth J.-M., Kaufmann R. and Schneider J. (1983), Solid State Comm. 46, 127
4. Hage J., Niklas J.R. and Spaeth J.-M. (1986), to be published
5. Niklas J.R. and Spaeth J.-M. (1980). phys. stat. sol. (b), 101, 221
6. Niklas J.R., Bauer R.U. and Spaeth J.-M. (1983), phys. stat. sol. (b) 119, 171
7. Cavenett B.C. (1981). Adv. Phys. 30, 475
8. Mollenauer L.F., Pan S. and Yngvesson S. (1969), Phys. Rev. Letts. 23, 689
9. Meyer B.K., Spaeth J.-M. and Scheffler M. (1984). Phys. Rev. Letts. 52, 851
10. Hofmann D.M., Meyer B.K., Lohse F. and Spaeth J.-M. (1984). Phys. Rev. Letts. 53, 1187
11. Seidel H. (1961). Z. Physik 165, 218
12. Pake G.E. and Estle T.L., The physical principles of electron paramagnetic resonance, Benjamin Inc., Reading Mass. (1973)
13. Spaeth J.-M. in: Defects and their structure in nonmetallic solids, Ed. B. Henderson and A.E. Hughes, Plenum Press, N.Y., 1976, p.155
14. Bromba M.U.A. and Ziegler H. (1984). Anal. Chem. 56, 2052
15. Niklas J.R., 1983, Habilitationsschrift, Paderborn
16. Kennedy T.A. and Wilsey N.D. (1978). Phys. Rev. Letts. 41, 977
17. Kennedy T.A., Wilsey N.D., Krebs J.J. and Stauss G.H. (1983). Phys. Rev. Letts. 50, 1281
18. Feuchtwang T.E. (1962). Phys. Rev. 126, 1628
19. Henry C.H. and Slichter C.P. (1968), in: Physics of Color Centers, Chapter 6, Ed. by W.B. Fowler, Acad. Press, N.Y.
20. Meyer B.K. and Spaeth J.-M. (1985). J. Phys. C: Solid State Phys. 18, L99
21. Spaeth J.-M., Hofmann D.M. and Meyer B.K. (1985). MRS Symposia Proc. 46, 185
22. Meyer B.K., Hofmann D.M. and Spaeth J.-M. (1986), to be published
23. Ahlers F.J., Lohse F., Spaeth J.-M. and Mollenauer L.F. (1983). Phys. Rev. B28, 1249
24. Meyer B.K. and Spaeth J.-M. (1986), to be published.